

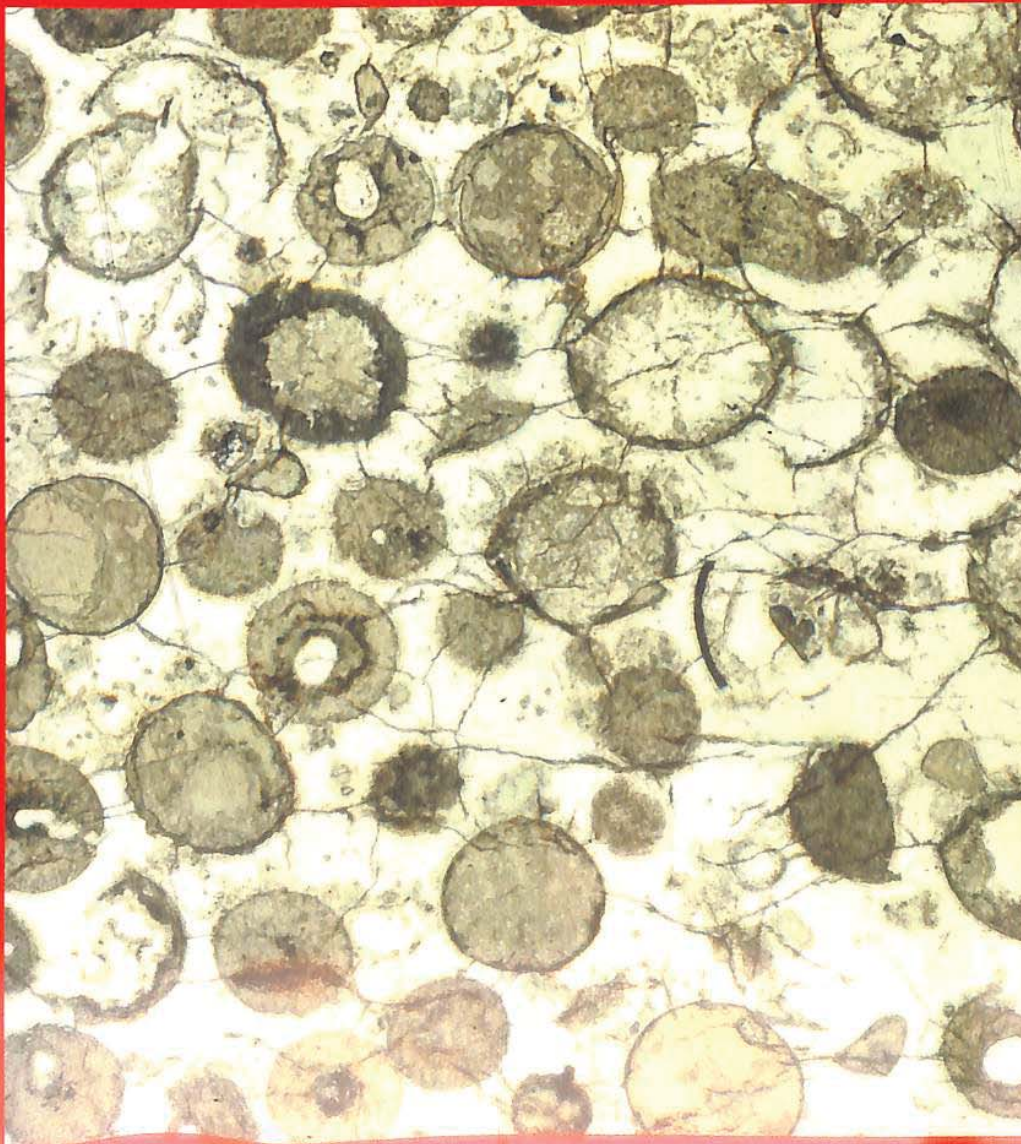


Volume 256

January 2015

ISSN 0301-9268

PRECAMBRIAN RESEARCH



(Abstracts/contents lists published in *Am. Geol. Inst. Bibliogr.*; *Abstr. Bull. Signalétique*; *Chem. Abstr.*; *Curr. Contents*; *Phys. Chem. Earth Sci.*; *Geo Abstr.*; *Mineral Abstr.*)

Salt domes of the UAE and Oman: Probing eastern Arabia R.J. Thomas, R.A. Ellison, K.M. Goodenough, N.M.W. Roberts and P.A. Allen	1
Geochronological and geochemical evidence for the nature of the Dongling Complex in South China S.-B. Zhang, Q. He and Y.-F. Zheng	17
Granulite-facies metamorphic events in the northwestern Ubendian Belt of Tanzania: Implications for the Neoproterozoic to Paleoproterozoic crustal evolution E.O. Kazimoto, V. Schenk and P. Appel	31
Involvement of fluids in the metamorphic processes within different zones of the Southern Marginal Zone of the Limpopo complex, South Africa: An oxygen isotope perspective E.O. Dubinina, L.Y. Aranovich, D.D. van Reenen, A.S. Avdeenko, D.A. Varlamov, V.V. Shaposhnikov and E.B. Kurdyukov	48
Geochemical and Sm-Nd isotopic characteristics of the Late Archaean-Palaeoproterozoic Dhanjori and Chaibasa metasedimentary rocks, Singhbhum craton, E. India: Implications for provenance, and contemporary basin tectonics S. De, R. Mazumder, T. Ohta, E. Hegner, K. Yamada, T. Bhattacharyya, J. Chiarenzelli, W. Altermann and M. Arima	62
A long-lived magma chamber in the Paleoproterozoic North China Craton: Evidence from the Damiao gabbro-anorthosite suite X. Teng and M. Santosh	79
New geochronological and Sm-Nd constraints across the Pajala shear zone of northern Fennoscandia: Reactivation of a Paleoproterozoic suture R. Lahtinen, H. Huhma, Y. Lahaye, E. Jonsson, T. Manninen, L.S. Lauri, S. Bergman, F. Hellström, T. Niiranen and M. Nironen	102
Palaeoproterozoic volcanism and granitic magmatism in the Ngualla area of the Ubendian Belt, SW Tanzania: Constraints from SHRIMP U-Pb zircon ages, and Sm-Nd isotope systematics T. Tulibonywa, S. Manyá and M.A.H. Maboko	120
Single zircon Hf-O isotope constraints on the origin of A-type granites from the Jabal Al-Hassir ring complex, Saudi Arabia K.A. Ali, A.A. Surour, M.J. Whitehouse and A. Andresen	131
A juvenile accretion episode (2.35–2.32 Ga) in the Mineiro belt and its role to the Minas accretionary orogeny: Zircon U-Pb-Hf and geochemical evidences W. Teixeira, C.A. Ávila, I.A. Dussin, A.V. Corrêa Neto, E.M. Bongiolo, J.O. Santos and N.S. Barbosa	148
Petrology, mineralogy and geochemical climofunctions of the Neoproterozoic Baltic paleosol S. Liivamägi, P. Somelar, I. Vircava, W.C. Mahaney, J. Kirs and K. Kirsimäe	170

(Contents continued on BM I)

CAPTION FOR COVER PHOTOGRAPH

3,243 million-year-old spherules in the Fig Tree Group, Barberton Greenstone Belt, South Africa, formed as a result of large meteorite impacts on the early Earth. The 35-cm-thick spherule bed (S3) is composed of nearly pure spherules produced during the condensation of an impact-produced rock vapor cloud. The estimated diameter of the bolide was 20–50 km. The spherules, 0.5–1.5 mm in diameter in the photo, include silica-(clear), phyllosilicate- (gray), and rutile/anatase-rich (black) varieties; massive and layered types; and a few originally hollow spherules. This is one of four spherule layers in the Barberton Belt, ranging from 3,470–3,243 Ma, that represent the oldest known impact deposits and provide direct evidence for a significant flux of large impactors as late as 3.2 Ga. Photograph: D.R. Lowe



(Contents continued from back cover)

Constrains on vorticity and non-coaxial shear direction in Neoproterozoic L-S tectonites, an example from northern Minnesota, USA J.E. Dyess, V.L. Hansen and C. Goscinak	189
Kotuikan Formation assemblage: A diverse organic-walled microbiota in the Mesoproterozoic Anabar succession, northern Siberia N.G. Vorob'eva, V.N. Sergeev and P.Yu. Petrov	201
Metamorphic evolution and Zircon ages of Garnet-orthoamphibole rocks in southern Hengshan, North China Craton: Insights into the regional Paleoproterozoic <i>P-T-t</i> history J. Qian, C. Wei, G.L. Clarke and X. Zhou	223
Petrogenesis of the 2.1 Ga Lushan garnet-bearing quartz monzonite on the southern margin of the North China Craton and its tectonic implications Y.-Y. Zhou, T.-P. Zhao, M.-G. Zhai, J.-F. Gao, Z.-W. Lan and Q.-Y. Sun	241
Geochronology and geochemistry of Cryogenian gabbros from the Ambatondrazaka area, east-central Madagascar: Implications for Madagascar-India correlation and Rodinia paleogeography J.-L. Zhou, S. Shao, Z.-H. Luo, J.-B. Shao, D.-T. Wu and V. Rasoamalala	256
Zircon provenance in meta-sandstones of the São Roque Domain: Implications for the Proterozoic evolution of the Ribeira Belt, SE Brazil R. Henrique-Pinto, V.A. Janasi, A.C.B.C. Vasconcellos, E.W. Sawyer, S.-J. Barnes, M.A.S. Basei and C.C.G. Tassinari	271
Paleoproterozoic record of the detrital pyrite-bearing, Jacobina Au-U deposits, Bahia, Brazil G. Teles, F. Chemale Jr. and C.G. de Oliveira	289
Sedimentology of the Paleoproterozoic Kungarra Formation, Turee Creek Group, Western Australia: A conformable record of the transition from early to modern Earth M.J. Van Kranendonk, R. Mazumder, K.E. Yamaguchi, K. Yamada and M. Ikehara	314
Corrigendum to "Did large volcanic channel systems develop on Earth during the Hadean and Archean?" [Precambrian Res. 246 (2014) 226-239] D.W. Leverington	344

(Abstracts/contents lists published in *Am. Geol. Inst. Bibliogr.*; *Abstr. Bull. Signalétique*; *Chem. Abstr.*; *Curr. Contents*; *Phys. Chem. Earth Sci.*; *Geo Abstr.*; *Mineral Abstr.*)

Mesoproterozoic delta systems of the Açuruá Formation, Chapada Diamantina, Brazil A.J.C. Magalhães, C.M.S. Scherer, G.P. Raja Gabaglia and O. Catuneanu	1
Tectono-metamorphic history of the eastern Taureau shear zone, Mauricie area, Québec: Implications for the exhumation of the mid-crust in the Grenville Province R. Soucy La Roche, F. Gervais, A. Tremblay, J.L. Crowley and G. Ruffet	22
The 600–580 Ma continental rift basalts in North Qilian Shan, northwest China: Links between the Qilian-Qaidam block and SE Australia, and the reconstruction of East Gondwana X. Xu, S. Song, L. Su, Z. Li, Y. Niu and M.B. Allen	47
Recognition and tectonic implications of an extensive Neoproterozoic volcano-sedimentary rift basin along the southwestern margin of the Tarim Craton, northwestern China C. Wang, L. Liu, Y.-H. Wang, S.-P. He, R.-S. Li, M. Li, W.-Q. Yang, Y.-T. Cao, A.S. Collins, C. Shi and Z.-N. Wu	65
Metasaprolite in the McGrath Gneiss, Minnesota, USA: Viewing Paleoproterozoic weathering through a veil of metamorphism and metasomatism L.G. Medaris Jr., T.J. Boerboom, B.R. Jicha and B.S. Singer	83
Heterogeneous redox conditions and a shallow chemocline in the Mesoproterozoic ocean: Evidence from carbon–sulfur–iron relationships G.J. Gilleaudeau and L.C. Kah	94
Late Archaean tidalites from western margin of Chitradurga greenstone belt, southern India H.N. Bhattacharya, B. Bhattacharya, S. Pal and A. Roy	109
Nature of 1800–1600 Ma mafic dyke swarms in the North China Craton: Implications for the rejuvenation of the sub-continental lithospheric mantle Y. Li, P. Peng, X. Wang and H. Wang	114
Taphonomy and morphology of the Ediacara form genus <i>Aspidella</i> L.G. Tarhan, M.L. Droser, J.G. Gehling and M.P. Dzaugis	124
A paleomagnetic and U–Pb geochronology study of the western end of the Grenville dyke swarm: Rapid changes in paleomagnetic field direction at ca. 585 Ma related to polarity reversals? H.C. Halls, A. Lovette, M. Hamilton and U. Söderlund	137

CAPTION FOR COVER PHOTOGRAPH

3,243 million-year-old spherules in the Fig Tree Group, Barberton Greenstone Belt, South Africa, formed as a result of large meteorite impacts on the early Earth. The 35-cm-thick spherule bed (S3) is composed of nearly pure spherules produced during the condensation of an impact-produced rock vapor cloud. The estimated diameter of the bolide was 20–50 km. The spherules, 0.5–1.5 mm in diameter in the photo, include silica-(clear), phyllosilicate- (gray), and rutile/anatase-rich (black) varieties; massive and layered types; and a few originally hollow spherules. This is one of four spherule layers in the Barberton Belt, ranging from 3,470–3,243 Ma, that represent the oldest known impact deposits and provide direct evidence for a significant flux of large impactors as late as 3.2 Ga. Photograph: D.R. Lowe



(Abstracts/contents lists published in *Am. Geol. Inst. Bibliogr.*; *Abstr. Bull. Signalétique*; *Chem. Abstr.*; *Curr. Contents*; *Phys. Chem. Earth Sci.*; *Geo Abstr.*; *Mineral Abstr.*)

Neoproterozoic arc–juvenile back-arc magmatism in eastern Dharwar Craton, India: Geochemical fingerprints from the basalts of Kadiri greenstone belt C. Manikyamba, S. Ganguly, M. Santosh, A. Saha, A. Chatterjee and A.C. Khelen	1
Micro-scale quadruple sulfur isotope analysis of pyrite from the ~3480 Ma Dresser Formation: New insights into sulfur cycling on the early Earth D. Wacey, N. Noffke, J. Cliff, M.E. Barley and J. Farquhar	24
Decline in oceanic sulfate levels during the early Mesoproterozoic G. Luo, S. Ono, J. Huang, T.J. Algeo, C. Li, L. Zhou, A. Robinson, T.W. Lyons and S. Xie	36
The evolving nature of terrestrial crust from the Hadean, through the Archaean, into the Proterozoic B.S. Kamber	48
A hidden Tonian basement in the eastern Mediterranean: Age constraints from U–Pb data of magmatic and detrital zircons of the External Hellenides (Crete and Peloponnesus) W. Dörr, G. Zulauf, A. Gerdes, Y. Lahaye and G. Kowalczyk	83
The Nhlngano gneiss dome in south-west Swaziland – A record of crustal destabilization of the eastern Kaapvaal craton in the Neoproterozoic A. Hofmann, A. Kröner, H. Xie, E. Hegner, G. Belyanin, J. Kramers, R. Bolhar, A. Slabunov, J. Reinhardt and P. Horváth	109
Detrital zircon U–Pb dating and whole-rock geochemistry from the clastic rocks in the northern marginal basin of the North China Craton: Constraints on depositional age and provenance of the Bayan Obo Group Y. Zhong, M. Zhai, P. Peng, M. Santosh and X. Ma	133
Mesoarchaean collision of Kapisilik terrane 3070 Ma juvenile arc rocks and >3600 Ma Isukasia terrane continental crust (Greenland) A.P. Nutman, V.C. Bennett, C.R.L. Friend, K. Yi and S.R. Lee	146
A marine to fluvial transition in the Paleoproterozoic Koolbye Formation, Turee Creek Group, Western Australia R. Mazumder, M.J. Van Kranendonk and W. Altermann	161
The geological composition of the hidden Wilhelm II Land in East Antarctica: SHRIMP zircon, Nd isotopic and geochemical studies with implications for Proterozoic supercontinent reconstructions E.V. Mikhalsky, B.V. Belyatsky, S.L. Presnyakov, S.G. Skublov, V.P. Kovach, N.V. Rodionov, A.V. Antonov, A.K. Saltykova and S.A. Sergeev	171
Detrital zircon ages and Nd isotope compositions of the Seridó and Lavras da Mangabeira basins (Borborema Province, NE Brazil): Evidence for exhumation and recycling associated with a major shift in sedimentary provenance M.H.B.M. Hollanda, C.J. Archanjo, J.R. Bautista and L.C. Souza	186
Neoproterozoic continental arc volcanism at the northern edge of the Arabian Plate, SE Turkey S. Gürsu, A. Möller, M.C. Göncüoğlu, S. Köksal, H. Demircan, F.T. Köksal, H. Kozlu and G. Sunal	208

(Contents continued on BM I)

CAPTION FOR COVER PHOTOGRAPH

3,243 million-year-old spherules in the Fig Tree Group, Barberton Greenstone Belt, South Africa, formed as a result of large meteorite impacts on the early Earth. The 35-cm-thick spherule bed (S3) is composed of nearly pure spherules produced during the condensation of an impact-produced rock vapor cloud. The estimated diameter of the bolide was 20–50 km. The spherules, 0.5–1.5 mm in diameter in the photo, include silica-(clear), phyllosilicate- (gray), and rutile/anatase-rich (black) varieties; massive and layered types; and a few originally hollow spherules. This is one of four spherule layers in the Barberton Belt, ranging from 3,470–3,243 Ma, that represent the oldest known impact deposits and provide direct evidence for a significant flux of large impactors as late as 3.2 Ga. Photograph: D.R. Lowe



(Contents continued from back cover)

Sm–Nd and Rb–Sr isotope geochemistry and petrology of Abu Hamamid intrusion, Eastern Desert, Egypt: An Alaskan-type complex in a backarc setting H.M. Helmy, M. Yoshikawa, T. Shibata, S. Arai and H. Kagami	234
The 2.65 Ga A-type granite in the northeastern Yangtze craton: Petrogenesis and geological implications G. Zhou, Y. Wu, S. Gao, J. Yang, J. Zheng, Z. Qin, H. Wang and S. Yang	247
Petrogenesis of basalt–high-Mg andesite–adakite in the Neoproterozoic Veligallu greenstone terrane: Geochemical evidence for a rifted back-arc crust in the eastern Dharwar craton, India T.C. Khanna, V.V. Sessa Sai, M. Bizimis and A.K. Krishna	260
Corrigendum to “Constraints on vorticity and non-coaxial shear direction in Neoproterozoic L-S tectonites, an example from northern Minnesota, USA” [Precambrian Res. 256 (2015) 189–200] J.E. Dyess, V.L. Hansen and C. Gosciniak	278



ELSEVIER

Contents lists available at ScienceDirect

Precambrian Research

journal homepage: www.elsevier.com/locate/precamres

Contents

Special Issue

Supercontinental Cycles and Geodynamics

Guest Editors:

Sergei A. Pisarevsky

Svetlana V. Bogdanova

Natalia V. Lubnina

J. Brendan Murphy

Preface

S.A. Pisarevsky, S.V. Bogdanova, N.V. Lubnina and J.B. Murphy 1

Eurasian cratons in Precambrian supercontinents

Trans-Baltic Palaeoproterozoic correlations towards the reconstruction of supercontinent Columbia/Nuna

S. Bogdanova, R. Gorbatshev, G. Skridlaite, A. Soesoo, L. Taran and D. Kurlovich 5

Is the Proterozoic Ladoga Rift (SE Baltic Shield) a rift?

I.M. Artemieva and A. Shulgin 34

The 2.31 Ga mafic dykes in the Karelian Craton, eastern Fennoscandian shield: U-Pb age, source characteristics and implications for continental break-up processes

A.V. Stepanova, E.B. Salnikova, A.V. Samsonov, S.V. Egorova, Y.O. Larionova and V.S. Stepanov 43

Paleomagnetism of the Ulkan massif (SE Siberian platform) and the apparent polar wander path for Siberia in late Paleoproterozoic-early Mesoproterozoic times

A.N. Didenko, V.Yu. Vodovozov, A.Yu. Peskov, V.A. Guryanov and A.V. Kosynkin 58

Proterozoic supercontinental restorations: Constraints from provenance studies of Mesoproterozoic to Cambrian clastic rocks, eastern Siberian Craton

A. Khudoley, K. Chamberlain, V. Ershova, J. Sears, A. Prokopiev, J. MacLean, G. Kazakova, S. Malyshev, A. Molchanov, K. Kullerud, J. Toro, E. Miller, R. Veselovskiy, A. Li and D. Chipley 78

Meso-Neoproterozoic petroleum systems of the Eastern Siberian sedimentary basins

S.V. Frolov, G.G. Akhmanov, E.A. Bakay, N.V. Lubnina, N.I. Korobova, E.E. Karnyushina and E.V. Kozlova 95

Arctida between Rodinia and Pangea

D.V. Metelkin, V.A. Vernikovskiy and N.Yu. Matushkin 114

New paleomagnetic results from the Ediacaran Doushantuo Formation in South China and their paleogeographic implications

S. Zhang, H. Li, G. Jiang, D.A.D. Evans, J. Dong, H. Wu, T. Yang, P. Liu and Q. Xiao 130

Building blocks of Gondwana in Precambrian supercontinents

The late Neoproterozoic Sierra de las Ánimas Magmatic Complex and Playa Hermosa Formation, southern Uruguay, revisited: Paleogeographic implications of new paleomagnetic and precise geochronologic data

A.E. Rapalini, E. Tohver, L.S. Bettucci, A.C. Lossada, H. Barcelona and C. Pérez 143

New insights on proterozoic tectonics and sedimentation along the peri-Gondwanan West African margin based on zircon U-Pb SHRIMP geochronology

B. De Waele, M. Lacorde, F. Vergara and G. Chan 156

The four Neoproterozoic glaciations of southern Namibia and their detrital zircon record: The fingerprints of four crustal growth events during two supercontinent cycles

M. Hofmann, U. Linnemann, K.-H. Hoffmann, G. Germs, A. Gerdes, L. Marko, K. Eckelmann, A. Gärtner and R. Krause 176

Early Neoproterozoic metagabbro-tonalite-trondhjemite of Sør Rondane (East Antarctica): Implications for supercontinent assembly	
M. Elburg, J. Jacobs, T. Andersen, C. Clark, A. Läufer, A. Ruppel, N. Krohne and D. Damaske	189
Western Australia-Kalahari (WAlahari) connection in Rodinia: Not supported by U/Pb detrital zircon data from the Maud Belt (East Antarctica) and the Northampton Complex (Western Australia)	
A.K. Ksienzyk and J. Jacobs	207
Paleomagnetism and U-Pb age of the 2.4 Ga Erayinia mafic dykes in the south-western Yilgarn, Western Australia: Paleogeographic and geodynamic implications	
S.A. Pisarevsky, B. De Waele, S. Jones, U. Söderlund and R.E. Ernst	222
Early history of the Amadęs Basin: Implications for the existence and geometry of the Centralian Superbasin	
A. Camacho, R. Armstrong, D.W. Davis and A. Bekker	232
Some implications of supercontinental cycles	
Mantle plumes, supercontinents, intracontinental rifting and mineral systems	
F. Pirajno and M. Santosh	243
The history of supercontinents and oceans from the standpoint of thermochemical mantle convection	
L. Lobkovsky and V. Kotelkin	262
Is the rate of supercontinent assembly changing with time?	
K. Condie, S.A. Pisarevsky, J. Korenaga and S. Gardoll	278

(Abstracts/contents lists published in *Am. Geol. Inst. Bibliogr.*; *Abstr. Bull. Signalétique*; *Chem. Abstr.*; *Curr. Contents*; *Phys. Chem. Earth Sci.*; *Geo Abstr.*; *Mineral Abstr.*)

Diachronic collision, slab break-off and long-term high thermal flux in the Brasiliano–Pan-African orogeny: Implications for the geodynamic evolution of the Mantiqueira Province T.M. Bento dos Santos, C.C.G. Tassinari and P.E. Fonseca	1
Geochronology and geochemistry of the Nanfen iron deposit in the Anshan-Benxi area, North China Craton: Implications for ~2.55 Ga crustal growth and the genesis of high-grade iron ores M. Zhu, Y. Dai, L. Zhang, C. Wang and L. Liu	23
²⁰⁷ Pb/ ²⁰⁶ Pb ages and Hf isotope composition of zircons from sedimentary rocks of the Ukrainian shield: Crustal growth of the south-western part of East European craton from Archaean to Neoproterozoic L. Shumlyanskyy, C. Hawkesworth, B. Dhuime, K. Billström, S. Claesson and C. Storey	39
Temperature–time evolution of the Assynt Terrane of the Lewisian Gneiss Complex of Northwest Scotland from zircon U–Pb dating and Ti thermometry J.M. MacDonald, K.M. Goodenough, J. Wheeler, Q. Crowley, S.L. Harley, E. Mariani and D. Tatham	55
Provenance and depositional age of Paleoproterozoic metasedimentary rocks in the Kuluketage Block, northern Tarim Craton: Implications for tectonic setting and crustal growth X. Long, S.A. Wilde, C. Yuan, A. Hu and M. Sun	76
In situ U–Pb geochronology of xenotime and monazite from the Abra polymetallic deposit in the Capricorn Orogen, Australia: Dating hydrothermal mineralization and fluid flow in a long-lived crustal structure J.-W. Zi, B. Rasmussen, J.R. Muhling, I.R. Fletcher, A.M. Thorne, S.P. Johnson, H.N. Cutten, D.J. Dunkley and F.J. Korhonen	91
A review of volcanic-hosted massive sulfide (VHMS) mineralization in the Archaean Yilgarn Craton, Western Australia: Tectonic, stratigraphic and geochemical associations S.P. Hollis, C.J. Yeats, S. Wyche, S.J. Barnes, T.J. Ivanic, S.M. Belford, G.J. Davidson, A.J. Roache and M.T.D. Wingate	113
Architecture of the Neoproterozoic Jaguar VHMS deposit, Western Australia: Implications for prospectivity and the presence of depositional breaks S.M. Belford, G.J. Davidson, J. McPhie and R.R. Large	136
Corrigendum to “Magmatic and metamorphic history of Paleoarchean tonalite–trondhjemite–granodiorite (TTG) suite from the Singhbhum craton, eastern India” [Precambrian Res. 252 (2014) 180–190] D. Upadhyay, S. Chattopadhyay, E. Kooijman, K. Mezger and J. Berndt	161

CAPTION FOR COVER PHOTOGRAPH

3,243 million-year-old spherules in the Fig Tree Group, Barberton Greenstone Belt, South Africa, formed as a result of large meteorite impacts on the early Earth. The 35-cm-thick spherule bed (S3) is composed of nearly pure spherules produced during the condensation of an impact-produced rock vapor cloud. The estimated diameter of the bolide was 20–50 km. The spherules, 0.5–1.5 mm in diameter in the photo, include silica-(clear), phyllosilicate- (gray), and rutile/anatase-rich (black) varieties; massive and layered types; and a few originally hollow spherules. This is one of four spherule layers in the Barberton Belt, ranging from 3,470–3,243 Ma, that represent the oldest known impact deposits and provide direct evidence for a significant flux of large impactors as late as 3.2 Ga. Photograph: D.R. Lowe



(Abstracts/contents lists published in *Am. Geol. Inst. Bibliogr.*; *Abstr. Bull. Signalétique*; *Chem. Abstr.*; *Curr. Contents*; *Phys. Chem. Earth Sci.*; *Geo Abstr.*; *Mineral Abstr.*)

Evolution history of the Neoproterozoic eclogite-bearing complex of the Muya dome (Central Asian Orogenic Belt): Constraints from zircon U-Pb age, Hf and whole-rock Nd isotopes V.S. Shatsky, V.G. Malkovets, E.A. Belousova and S.Yu. Skuzovatov	1
New material of the biomineralizing tubular fossil <i>Sinotubulites</i> from the late Ediacaran Dengying Formation, South China Y. Cai, S. Xiao, H. Hua and X. Yuan	12
An integrated approach to the late stages of Neoproterozoic post-collisional magmatism from Southern Brazil: Structural geology, geochemistry and geochronology of the Corre-mar Granite A. Martini, M. de Fátima Bitencourt, L.V.S. Nardi and L.M. Florisbal	25
Neoproterozoic subduction-related metavolcanic and metasedimentary rocks from the Rey Bouba Greenstone Belt of north-central Cameroon in the Central African Fold Belt: New insights into a continental arc geodynamic setting M.H. Bouyo, Y. Zhao, J. Penaye, S.H. Zhang and U.O. Njel	40
High resolution tephra and U/Pb chronology of the 3.33-3.26 Ga Mendon Formation, Barberton Greenstone Belt, South Africa N.B. Decker, G.R. Byerly, M. Thompson Stiegler, D.R. Lowe and E. Stefurak	54
Mesoproterozoic continental growth: U-Pb-Hf-O zircon record in the Idefjorden Terrane, Sveconorwegian Orogen A. Petersson, A. Scherstén, B. Bingen, A. Gerdes and M.J. Whitehouse	75
Extreme ocean anoxia during the Late Cryogenian recorded in reefal carbonates of Southern Australia A. van Sameerdijk Hood and M.W. Wallace	96
Hf isotopes in detrital and inherited zircons of the Pilbara Craton provide no evidence for Hadean continents A.I.S. Kemp, A.H. Hickman, C.L. Kirkland and J.D. Vervoort	112
Archean-Proterozoic collision boundary in central Fennoscandia: Revisited R. Lahtinen, H. Huhma, Y. Lahaye, J. Kousa and J. Luukas	127
Analysis of the Ragged Basin, Western Australia: Insights into syn-orogenic basin evolution within the Albany-Fraser Orogen P.A. Waddell, N.E. Timms, C.V. Spaggiari, C.L. Kirkland and M.T.D. Wingate	166
Charnokite magmatism during a transitional phase: Implications for late Paleoproterozoic ridge subduction in the North China Craton Q.-Y. Yang and M. Santosh	188
Temporal, environmental and tectonic significance of the Huoqiu BIF, southeastern North China Craton: Geochemical and geochronological constraints L. Liu and X. Yang	217
Ediacaran-Cambrian paleogeography and geodynamic setting of the Central Iberian Zone: Constraints from coupled U-Pb-Hf isotopes of detrital zircons D. Orejana, E. Merino Martínez, C. Villaseca and T. Andersen	234

(Contents continued on BM I)

CAPTION FOR COVER PHOTOGRAPH

3,243 million-year-old spherules in the Fig Tree Group, Barberton Greenstone Belt, South Africa, formed as a result of large meteorite impacts on the early Earth. The 35-cm-thick spherule bed (S3) is composed of nearly pure spherules produced during the condensation of an impact-produced rock vapor cloud. The estimated diameter of the bolide was 20–50 km. The spherules, 0.5–1.5 mm in diameter in the photo, include silica-(clear), phyllosilicate- (gray), and rutile/anatase-rich (black) varieties; massive and layered types; and a few originally hollow spherules. This is one of four spherule layers in the Barberton Belt, ranging from 3,470–3,243 Ma, that represent the oldest known impact deposits and provide direct evidence for a significant flux of large impactors as late as 3.2 Ga. Photograph: D.R. Lowe



(Contents continued from back cover)

Dynamic redox conditions control late Ediacaran metazoan ecosystems in the Nama Group, Namibia R.A. Wood, S.W. Poulton, A.R. Prave, K.-H. Hoffmann, M.O. Clarkson, R. Guilbaud, J.W. Lyne, R. Tostevin, F. Bowyer, A.M. Penny, A. Curtis and S.A. Kasemann	252
Pre-Sturtian (800-730 Ma) depositional age of carbonates in sedimentary sequences hosting stratiform iron ores in the Uppermost Allochthon of the Norwegian Caledonides: A chemostratigraphic approach V.A. Melezhik, P.M. Ihlen, A.B. Kuznetsov, S. Gjelle, A. Solli, I.M. Gorokhov, A.E. Fallick, J.S. Sandstad and T. Bjerkgård	272

(Abstracts/contents lists published in *Am. Geol. Inst. Bibliogr.*; *Abstr. Bull. Signalétique*; *Chem. Abstr.*; *Curr. Contents*; *Phys. Chem. Earth Sci.*; *Geo Abstr.*; *Mineral Abstr.*)

Charnockites and UHT metamorphism in the Bakhuis Granulite Belt, western Suriname: Evidence for two separate UHT events M. Klaver, E.W.F. de Roever, J.A.M. Nanne, P.R.D. Mason and G.R. Davies	1
Hypozonal lode gold deposits: A genetic concept based on a review of the New Consort, Renco, Hutti, Hira Buddini, Navachab, Nevoria and The Granites deposits J. Kolb, A. Dziggel and L. Bagas	20
Giant gas discovery in the Precambrian deeply buried reservoirs in the Sichuan Basin, China: Implications for gas exploration in old cratonic basins G. Zhu, T. Wang, Z. Xie, B. Xie and K. Liu	45
Potassium metasomatism of Precambrian paleosols A.A. Novoselov and C.R. de Souza Filho	67
Neoproterozoic arc-related andesite and orogeny-related unconformity in the eastern Jiangnan orogenic belt: Constraints on the assembly of the Yangtze and Cathaysia blocks in South China J. Yao, L. Shu, M. Santosh and J. Li	84
The Kivalliq Igneous Suite: Anorogenic bimodal magmatism at 1.75 Ga in the western Churchill Province, Canada T.D. Peterson, J.M.J. Scott, A.N. LeCheminant, C.W. Jefferson and S.J. Pehrsson	101
Corrigendum to "Detrital zircon ages and Nd isotope compositions of the Seridó and Lavras da Mangabeira basins (Borborema Province, NE Brazil): Evidence for exhumation and recycling associated with a major shift in sedimentary provenance" [Precambrian Res. 258 (2015) 186–207] M.H.B.M. Hollanda, C.J. Archanjo, J.R. Bautista and L.C. Souza	120
Corrigendum to "Geochemical and Sm–Nd isotopic characteristics of the Late Archaean–Palaeoproterozoic Dhanjori and Chaibasa metasedimentary rocks, Singhbhum craton, E. India: Implications for provenance, and contemporary basin tectonics" [Precambrian Res. 256 (2015) 62–78] S. De, R. Mazumder, T. Ohta, E. Hegner, K. Yamada, T. Bhattacharyya, J. Chiarenzelli, W. Altermann and M. Arima	121
Letters to Editor	
Nature of Cryogenian felsic igneous rocks in Madagascar reevaluated: A comment on "From passive margin to volcano-sedimentary forearc: The Tonian to Cryogenian evolution of the Anosyen Domain of southeastern Madagascar" by Boger et al. J.-L. Zhou.....	123
Reply to comment by J-L Zhou on "From passive margin to volcano-sedimentary forearc: The Tonian to Cryogenian evolution of the Anosyen Domain of southeastern Madagascar" by Boger et al. Precambrian Research, Volume 247, July 2014, Pages 159–186 S.D. Boger, W. Hirdes, C.A.M. Ferreira, B. Schulte, T. Jenett and C.M. Fanning	127

CAPTION FOR COVER PHOTOGRAPH

3,243 million-year-old spherules in the Fig Tree Group, Barberton Greenstone Belt, South Africa, formed as a result of large meteorite impacts on the early Earth. The 35-cm-thick spherule bed (S3) is composed of nearly pure spherules produced during the condensation of an impact-produced rock vapor cloud. The estimated diameter of the bolide was 20–50 km. The spherules, 0.5–1.5 mm in diameter in the photo, include silica-(clear), phyllosilicate- (gray), and rutile/anatase-rich (black) varieties; massive and layered types; and a few originally hollow spherules. This is one of four spherule layers in the Barberton Belt, ranging from 3,470–3,243 Ma, that represent the oldest known impact deposits and provide direct evidence for a significant flux of large impactors as late as 3.2 Ga. Photograph: D.R. Lowe



(Abstracts/contents lists published in *Am. Geol. Inst. Bibliogr.*; *Abstr. Bull. Signalétique*; *Chem. Abstr.*; *Curr. Contents*; *Phys. Chem. Earth Sci.*; *Geo Abstr.*; *Mineral Abstr.*)

Periglacial paleosols and Cryogenian paleoclimate near Adelaide, South Australia G.J. Retallack, B.N. Gose and J.T. Osterhout	1
The marine environments encompassing the Neoproterozoic glaciations: Evidence from C, Sr and Fe isotope ratios in the Hecla Hoek Supergroup in Svalbard M. Tahata, Y. Sawaki, K. Yoshiya, M. Nishizawa, T. Komiya, T. Hirata, N. Yoshida, S. Maruyama and B.F. Windley	19
U–Pb zircon ages from volcanic and sedimentary rocks of the Ediacaran Bas Draâ inlier (Anti-Atlas Morocco): Chronostratigraphic and provenance implications B. Karaoui, C. Breitreuz, A. Mahmoudi, N. Youbi, M. Hofmann, A. Gärtner and U. Linnemann	43
Ediacaran biota in the aftermath of the Kotlinian Crisis: Asha Group of the South Urals A.V. Kolesnikov, V.V. Marusin, K.E. Nagovitsin, A.V. Maslov and D.V. Grazhdankin	59
Diagenetic barite deposits in the Yurtus Formation in Tarim Basin, NW China: Implications for barium and sulfur cycling in the earliest Cambrian X. Zhou, D. Chen, S. Dong, Y. Zhang, Z. Guo, H. Wei and H. Yu	79
Eoarchean ultra-depleted mantle domains inferred from ca. 3.81 Ga Anshan trondhjemitic gneisses, North China Craton Y.-F. Wang, X.-H. Li, W. Jin and J.-H. Zhang	88
New data of the Bayan Obo Fe–REE–Nb deposit, Inner Mongolia: Implications for ore genesis X. Lai, X. Yang, M. Santosh, Y. Liu and M. Ling	108
Revisiting the Liantuo Formation in Yangtze Block, South China: SIMS U–Pb zircon age constraints and regional and global significance Z. Lan, X.-H. Li, M. Zhu, Q. Zhang and Q.-L. Li	123
Assessing the veracity of Precambrian ‘sponge’ fossils using <i>in situ</i> nanoscale analytical techniques A.D. Muscente, F. Marc Michel, J.G. Dale and S. Xiao	142
Paleoproterozoic I-type granites and their implications for the Yangtze block position in the Columbia supercontinent: Evidence from the Lengshui Complex, South China Z. Wang, J. Wang, Q. Deng, Q. Du, X. Zhou, F. Yang and H. Liu	157
Mode of emplacement of Archean komatiitic tuffs and flows in the Selkirk Bay area, Melville Peninsula, Nunavut, Canada L. Richan, H.L. Gibson, M.G. Houlé and C.M. Leshner	174
Paleoproterozoic crustal growth in the North China Craton: Evidence from the Lüliang Complex M. Santosh, Q.-Y. Yang, X. Teng and L. Tang	197
Chemostratigraphy of the Shaler Supergroup, Victoria Island, NW Canada: A record of ocean composition prior to the Cryogenian glaciations D. Thomson, R.H. Rainbird, N. Planavsky, T.W. Lyons and A. Bekker	232
Sequence and tectonostratigraphy of the Neoproterozoic (Tonian–Cryogenian) Amundsen Basin prior to supercontinent (Rodinia) breakup D. Thomson, R.H. Rainbird and B. Krapez	246

CAPTION FOR COVER PHOTOGRAPH

3,243 million-year-old spherules in the Fig Tree Group, Barberton Greenstone Belt, South Africa, formed as a result of large meteorite impacts on the early Earth. The 35-cm-thick spherule bed (S3) is composed of nearly pure spherules produced during the condensation of an impact-produced rock vapor cloud. The estimated diameter of the bolide was 20–50 km. The spherules, 0.5–1.5 mm in diameter in the photo, include silica-(clear), phyllosilicate- (gray), and rutile/anatase-rich (black) varieties; massive and layered types; and a few originally hollow spherules. This is one of four spherule layers in the Barderton Belt, ranging from 3,470–3,243 Ma, that represent the oldest known impact deposits and provide direct evidence for a significant flux of large impactors as late as 3.2 Ga. Photograph: D.R. Lowe



(Abstracts/contents lists published in *Am. Geol. Inst. Bibliogr.*; *Abstr. Bull. Signalétique*; *Chem. Abstr.*; *Curr. Contents*; *Phys. Chem. Earth Sci.*, *Geo Abstr.*; *Mineral Abstr.*)

.A possible buried Paleoproterozoic collisional orogen beneath central South China: Evidence from seismic-reflection profiling S.W. Dong, Y.Q. Zhang, R. Gao, J.B. Su, M. Liu and J.H. Li	1
Geochemistry, zircon U–Pb geochronology and Hf isotopes of granitic rocks in the Xitieshan area, North Qaidam, Northwest China: Implications for Neoproterozoic geodynamic evolutions of North Qaidam J. Fu, X. Liang, Y. Zhou, C. Wang, Y. Jiang and Y. Zhong	11
Variations in the abundance of photosynthetic oxygen through Precambrian and Paleozoic time in relation to biotic evolution and mass extinctions: evidence from Mn/Fe ratios T.A. Jackson	30
Neoproterozoic subduction: A case study of arc volcanic rocks in Qinglong-Zhuzhangzi area of the Eastern Hebei Province, North China Craton R. Guo, S. Liu, D. Wyman, X. Bai, W. Wang, M. Yan and Q. Li	36
Imaging the basement architecture across the Cork Fault in Queensland using magnetic and gravity data G.P.T. Spampinato, L. Ailleres, P.G. Betts and R.J. Armit	63
Regional geodynamic context for the Mesoproterozoic Kibara Belt (KIB) and the Karagwe-Ankole Belt: Evidence from geochemistry and isotopes in the KIB D. Debryne, N. Hulsbosch, J. Van Wilderode, L. Balcaen, F. Vanhaecke and P. Muchez	82
Convergent margin magmatism and crustal evolution during Archean-Proterozoic transition in the Jiaobei terrane: Zircon U–Pb ages, geochemistry, and Nd isotopes of amphibolites and associated grey gneisses in the Jiaodong complex, North China Craton H. Shan, M. Zhai, E.P. Oliveira, M. Santosh and F. Wang	98
Two episodes of Paleoproterozoic mafic intrusions from Liaoning province, North China Craton: Petrogenesis and tectonic implications L. Yuan, X. Zhang, F. Xue, C. Han, H. Chen and M. Zhai	119
Geochemical constraints on the provenance and depositional setting of Neoproterozoic volcanoclastic rocks on the northern margin of the Yangtze Block, China: Implications for the tectonic evolution of the northern margin of the Yangtze Block Z. Xiang, Q. Yan, J.D.L. White, B. Song and Z. Wang	140
Metamorphism and geochronology of the Luoning metamorphic terrane, southern terminal of the Palaeoproterozoic Trans-North China Orogen, North China Craton H.-X. Chen, J. Wang, H. Wang, G.-D. Wang, T. Peng, Y.-H. Shi, Q. Zhang and C.-M. Wu	156
Evolution of Neoproterozoic Wonoka–Shuram Anomaly-aged carbonates: Evidence from clumped isotope paleothermometry S.J. Loyd, F.A. Corsetti, R.A. Eagle, J.W. Hagadorn, Y. Shen, X. Zhang, M. Bonifacie and A.K. Tripathi	179

(Contents continued on BM I)

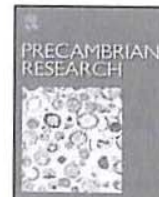
CAPTION FOR COVER PHOTOGRAPH

3,243 million-year-old spherules in the Fig Tree Group, Barberton Greenstone Belt, South Africa, formed as a result of large meteorite impacts on the early Earth. The 35-cm-thick spherule bed (S3) is composed of nearly pure spherules produced during the condensation of an impact-produced rock vapor cloud. The estimated diameter of the bolide was 20–50 km. The spherules, 0.5–1.5 mm in diameter in the photo, include silica-(clear), phyllosilicate- (gray), and rutile/anatase-rich (black) varieties; massive and layered types; and a few originally hollow spherules. This is one of four spherule layers in the Barberton Belt, ranging from 3,470–3,243 Ma, that represent the oldest known impact deposits and provide direct evidence for a significant flux of large impactors as late as 3.2 Ga. Photograph: D.R. Lowe



(Contents continued from back cover)

Tectonothermal history of the NE Jiangshan–Shaoxing suture zone: Evidence from $^{40}\text{Ar}/^{39}\text{Ar}$ and fission-track thermochronology in the Chencai region F. Wang, H. Chen, G.E. Batt, X. Lin, J. Gong, G. Gong, L. Meng, S. Yang and F. Jourdan	192
A duality of timescales: Short-lived ultrahigh temperature metamorphism preserving a long-lived monazite growth history in the Grenvillian Musgrave–Albany–Fraser Orogen N.M. Tucker, M. Hand, D.E. Kelsey and R.A. Dutch	204
Migmatization related to mafic underplating and intra- or back-arc spreading above a subduction boundary in a 2.0–1.8 Ga accretionary orogen, Sweden M.B. Stephens and J. Andersson	235



Contents

Special Issue

The structural, metamorphic and magmatic evolution of Mesoproterozoic orogens

Guest Editors:

Nick Roberts

Trond Slagstad

Giulio Viola

The structural, metamorphic and magmatic evolution of Mesoproterozoic orogens G. Viola, N. Roberts, T. Slagstad and R. Parrish	1
<i>Pre-Rodinia Orogenesis</i>	
Hollandian 1.45 Ga high-temperature metamorphism in Baltica: P-T evolution and SIMS U-Pb zircon ages of aluminous gneisses, SW Sweden J. Ulmius, J. Andersson and C. Möller	10
<i>Rodinia-forming Orogenesis</i>	
Detrital zircon signatures of the Baltoscandian margin along the Arctic Circle Caledonides in Sweden: The Sveconorwegian connection D.G. Gee, P.-G. Andréasson, H. Lorenz, D. Frei and J. Majka	40
The Late Mesoproterozoic Sirdal Magmatic Belt, SW Norway: Relationships between magmatism and metamorphism and implications for Sveconorwegian orogenesis N. Coint, T. Slagstad, N.M.W. Roberts, M. Marker, T. Røhr and B.E. Sørensen	57
Multiple reactivation and strain localization along a Proterozoic orogen-scale deformation zone: The Kongsberg-Telemark boundary in southern Norway revisited T. Scheiber, G. Viola, B. Bingen, M. Peters and A. Solli	78
High-temperature deformation in the basal shear zone of an eclogite-bearing fold nappe, Sveconorwegian orogen, Sweden L. Tual, A. Piñán-Llamas and C. Möller	104
Polyphasal foreland-vergent deformation in a deep section of the 1 Ga Sveconorwegian orogen A. Piñán Llamas, J. Andersson, C. Möller, L. Johansson and E. Hansen	121
Geochronological constraints on the Hartbees River Thrust and Augrabies Nappe: New insights into the assembly of the Mesoproterozoic Namaqua-Natal Province of Southern Africa W.P. Colliston, D.H. Cornell, A.E. Schoch and H.E. Praekelt	150
Geochronology of Mesoproterozoic hybrid intrusions in the Konkiep Terrane, Namibia, from passive to active continental margin in the Namaqua-Natal Wilson Cycle D.H. Cornell, V. van Schijndel, S.L. Simonsen and D. Frei	166
Geochronology of emplacement and charnockite formation of the Margate Granite Suite, Natal Metamorphic Province, South Africa: Implications for Natal-Maud belt correlations P. Mendonidis, R.J. Thomas, G.H. Grantham and R.A. Armstrong	189
Crustal growth during island arc accretion and transcurrent deformation, Natal Metamorphic Province, South Africa: New isotopic constraints C.J. Spencer, R.J. Thomas, N.M.W. Roberts, P.A. Cawood, I. Millar and S. Tapster	203
Foreign contemporaries - Unravelling disparate isotopic signatures from Mesoproterozoic Central and Western Australia C.L. Kirkland, R.H. Smithies and C.V. Spaggiari	218

Rapid cooling and exhumation in the western part of the Mesoproterozoic Albany-Fraser Orogen, Western Australia E. Scibiorski, E. Tohver and F. Jourdan	232
Two distinct Late Mesoproterozoic/Early Neoproterozoic basement provinces in central/eastern Dronning Maud Land, East Antarctica: The missing link, 15-21° E J. Jacobs, M. Elburg, A. Läufer, I.C. Kleinhanns, F. Henjes-Kunst, S. Estrada, A.S. Ruppel, D. Damaske, P. Montero and F. Bea	249
<i>Magmatism</i>	
Precise ID-TIMS U-Pb baddeleyite ages (1110-1112 Ma) for the Rincón del Tigre-Huanchaca large igneous province (LIP) of the Amazonian Craton: Implications for the Rodinia supercontinent W. Teixeira, M.A. Hamilton, G.A. Lima, A.S. Ruiz, R. Matos and R.E. Ernst	273
Mesoproterozoic-trans-Laurentian magmatism: A synthesis of continent-wide age distributions, new SIMS U-Pb ages, zircon saturation temperatures, and Hf and Nd isotopic compositions M.E. Bickford, W.R. Van Schmus, K.E. Karlstrom, P.A. Mueller and G.D. Kamenov	286
Zircon U-Pb, Hf and O isotope constraints on growth versus reworking of continental crust in the subsurface Grenville orogen, Ohio, USA A. Petersson, A. Scherstén, J. Andersson, M.J. Whitehouse and M.T. Baranoski	313

(Abstracts/contents lists published in *Am. Geol. Inst. Bibliogr.*; *Abstr. Bull. Signalétique*; *Chem. Abstr.*; *Curr. Contents*; *Phys. Chem. Earth Sci.*, *Geo Abstr.*; *Mineral Abstr.*)

The detrital zircon U-Pb-Hf fingerprint of the northern Arabian-Nubian Shield as reflected by a Late Ediacaran arkosic wedge (Zenifim Formation; subsurface Israel) D. Avigad, T. Weissbrod, A. Gerdes, O. Zlatkin, T.R. Ireland and N. Morag	1
Detrital zircon age patterns and provenance assessment for pre-glacial to post-glacial successions of the Neoproterozoic Macaúbas Group, Araçuaí orogen, Brazil M. Kuchenbecker, A.C. Pedrosa-Soares, M. Babinski and M. Fanning	12
Geochemical stratigraphy, sedimentology, and Mo isotope systematics of the ca. 2.58–2.50 Ga-old Transvaal Supergroup carbonate platform, South Africa S. Eroglu, R. Schoenberg, M. Wille, N. Beukes and H. Taubald	27
Morphological adaptations of 3.22 Ga-old tufted microbial mats to Archean coastal habitats (Moodies Group, Barberton Greenstone Belt, South Africa) M. Homann, C. Heubeck, A. Airo and M.M. Tice	47
Hualong Complex, South Qilian terrane: U-Pb and Lu-Hf constraints on Neoproterozoic micro-continental fragments accreted to the northern Proto-Tethyan margin Z. Yan, J. Aitchison, C. Fu, X. Guo, M. Niu, W. Xia and J. Li	65
Geochronology, mineralogy and geochemistry of alkali-feldspar granite and albite granite association from the Changyi area of Jiao-Liao-Ji Belt: Implications for Paleoproterozoic rifting of eastern North China Craton T.-G. Lan, H.-R. Fan, K.-F. Yang, Y.-C. Cai, B.-J. Wen and W. Zhang	86
Isotope (S-Sr-Nd-Pb) constraints on the genesis of the ca. 850 Ma Tumen Mo-F deposit in the Qinling Orogen, China X.-H. Deng, Y.-J. Chen, L. Bagas, H.-Y. Zhou, J.-M. Yao, Z. Zheng and P. Wang	108
Silica-undersaturated spinel granulites in the Daqingshan complex of the Khondalite Belt, North China Craton: Petrology and quantitative <i>P-T-X</i> constraints J. Cai, F. Liu, P. Liu, C. Liu, F. Wang and J. Shi	119
Neoproterozoic crustal growth of the Southern Yangtze Block: Geochemical and zircon U-Pb geochronological and Lu-Hf isotopic evidence of Neoproterozoic diorite from the Ailaoshan zone Y. Cai, Y. Wang, P.A. Cawood, Y. Zhang and A. Zhang	137
Fluid inclusion analysis of silicified Palaeoarchean oceanic crust - A record of Archaean seawater? K. Farber, A. Dziggel, F.M. Meyer, W. Prochaska, A. Hofmann and C. Harris	150
Mid-Neoproterozoic angular unconformity in the Yangtze Block revisited: Insights from detrital zircon U-Pb age and Hf-O isotopes C. Yang, X.-H. Li, X.-C. Wang and Z. Lan	165
Origin of the North Qinling Microcontinent and Proterozoic geotectonic evolution of the Kuanping Ocean, Central China Z. Zhang, S. Li, H. Cao, I.D. Somerville, S. Zhao and S. Yu	179

(Contents continued on BM I)

CAPTION FOR COVER PHOTOGRAPH

3,243 million-year-old spherules in the Fig Tree Group, Barberton Greenstone Belt, South Africa, formed as a result of large meteorite impacts on the early Earth. The 35-cm-thick spherule bed (S3) is composed of nearly pure spherules produced during the condensation of an impact-produced rock vapor cloud. The estimated diameter of the bolide was 20–50 km. The spherules, 0.5–1.5 mm in diameter in the photo, include silica-(clear), phyllosilicate- (gray), and rutile/anatase-rich (black) varieties; massive and layered types; and a few originally hollow spherules. This is one of four spherule layers in the Barberton Belt, ranging from 3,470–3,243 Ma, that represent the oldest known impact deposits and provide direct evidence for a significant flux of large impactors as late as 3.2 Ga. Photograph: D.R. Lowe



(Contents continued from back cover)

Sedimentology, chemostratigraphy, and stromatolites of lower Paleoproterozoic carbonates, Turee Creek Group, Western Australia R.C. Martindale, J.V. Strauss, E.A. Sperling, J.E. Johnson, M.J. Van Kranendonk, D. Flannery, K. French, K. Lepot, R. Mazumder, M.S. Rice, D.P. Schrag, R. Summons, M. Walter, J. Abelson and A.H. Knoll	194
Early deformation in the Eastern Goldfields, Yilgarn Craton, Western Australia: A record of early thrusting? L. Cohalan, R.F. Weinberg, R.J. Squire and C.M. Allen	212
Sedimentary petrology and detrital zircon U-Pb and Lu-Hf constraints of Mesoproterozoic intracratonic sequences in the Espinhaço Supergroup: Implications for the Archean and Proterozoic evolution of the São Francisco Craton F. Guadagnin, F. Chemale Junior, A.J.C. Magalhães, L. Alessandretti, M.B. Bállico and A.R. Jelinek	227
U-Pb and Sm-Nd isotopic constraints on the evolution of the Paleoproterozoic Peräpohja Belt, northern Finland J.-P. Ranta, L.S. Lauri, E. Hanski, H. Huhma, Y. Lahaye and E. Vanhanen	246
The affinity of Archean crust on the Yilgarn-Albany-Fraser Orogen boundary: Implications for gold mineralisation in the Tropicana Zone C.L. Kirkland, C.V. Spaggiari, R.H. Smithies, M.T.D. Wingate, E.A. Belousova, Y. Gréau, M.T. Sweetapple, R. Watkins, S. Tessalina and R. Creaser	260
Crustal velocity structure of the Neoproterozoic convergence zone between the eastern and western blocks of Dharwar Craton, India from seismic wide-angle studies V. Vijaya Rao, A.S.N. Murty, D. Sarkar, Y.J. Bhaskar Rao, P. Khare, A.S.S.R.S. Prasad, V. Sridher, S. Raju, G.S.P. Rao, Karuppanan, N. Prem Kumar and M.K. Sen	282
Organic-walled microfossils from the Tonian Gouhou Formation, Huaibei region, North China Craton, and their biostratigraphic implications Q. Tang, K. Pang, X. Yuan, B. Wan and S. Xiao	296
Sulfur isotope composition of carbonate-associated sulfate from the Mesoproterozoic Jixian Group, North China: Implications for the marine sulfur cycle H. Guo, Y. Du, L.C. Kah, C. Hu, J. Huang, H. Huang, W. Yu and H. Song	319
Unraveling the tectonic evolution of a Neoproterozoic-Cambrian active margin in the Ribeira Orogen (SE Brazil): U-Pb and Lu-Hf provenance data G.L. de F. Fernandes, R. da Silva Schmitt, E.M. Bongiolo, M.A.S. Basei and J.C. Mendes	337
Neoproterozoic-Early Cambrian biota and ancient niche: A synthesis from molecular markers and palynomorphs from Bikaner-Nagaur Basin, western India S. Bhattacharya and S. Dutta	361
The Neoproterozoic transition between medium- and high-K granitoids: Clues from the Southern São Francisco Craton (Brazil) F. Farina, C. Albert and C. Lana	375
Paleomagnetic and cyclostratigraphic constraints on the synchronicity and duration of the Shuram carbon isotope excursion, Johnnie Formation, Death Valley Region, CA D. Minguez, K.P. Kodama and J.W. Hillhouse	395
Geochemical and geochronological evidence for a former early Neoproterozoic microcontinent in the South Beishan Orogenic Belt, southernmost Central Asian Orogenic Belt Y. Yuan, K. Zong, Z. He, R. Klemd, Y. Liu, Z. Hu, J. Guo and Z. Zhang	409
Multiple post-Svecofennian 1750-1560 Ma pegmatite dykes in Archaean-Palaeoproterozoic rocks of the West Troms Basement Complex, North Norway: Geological significance and regional implications S.G. Bergh, F. Corfu, N. Priyatkinina, K. Kullerud and P.I. Myhre	425
Transformation of an Archean craton margin during Proterozoic basin formation and magmatism: The Albany-Fraser Orogen, Western Australia C.V. Spaggiari, C.L. Kirkland, R.H. Smithies, M.T.D. Wingate and E.A. Belousova	440
Early Neoproterozoic arc magmatism in the Lützow-Holm Complex, East Antarctica: Petrology, geochemistry, zircon U-Pb geochronology and Lu-Hf isotopes and tectonic implications T. Tsunogae, Q.-Y. Yang and M. Santosh	467
A 2082 Ma radiating dyke swarm in the Eastern Dharwar Craton, southern India and its implications to Cuddapah basin formation A. Kumar, V. Parashuramulu and E. Nagaraju	490
Proto-India was a part of Rodinia: Evidence from Grenville-age suturing of the Eastern Ghats Province with the Paleoproterozoic Singhbhum Craton S. Chattopadhyay, D. Upadhyay, J.K. Nanda, K. Mezger, K.L. Pruseth and J. Berndt	506
Geochemistry and age of mafic rocks from the Votuverava Group, southern Ribeira Belt, Brazil: Evidence for 1490 Ma oceanic back arc magmatism G.A.C. Campanha, F.M. Faleiros, M.A.S. Basei, C.C.G. Tassinari, A.P. Nutman and P.M. Vasconcelos	530
Ages and tectonic implications of Neoproterozoic ortho- and paragneisses in the Beishan Orogenic Belt, China Q. Liu, G. Zhao, M. Sun, P.R. Eisenhöfer, Y. Han, W. Hou, X. Zhang, B. Wang, D. Liu and B. Xu	551

Large variations in lithospheric thickness of western Laurentia: Tectonic inheritance or collisional reworking? 579
X. Bao and D.W. Eaton
Changing tectonic settings through time: Indiscriminate use of geochemical discriminant diagrams 587
K. Condie
Corrigendum to "A paleomagnetic and U-Pb geochronology study of the western end of the Grenville dyke swarm:
Rapid changes in paleomagnetic field direction at ca. 585 Ma related to polarity reversals?" [Precambrian Res.
257 (2015) 137-166]
H.C. Halls, A. Lovette, M. Hamilton and U. Söderlund 592



(Abstracts/contents lists published in *Am. Geol. Inst. Bibliogr.*; *Abstr. Bull. Signalétique*; *Chem. Abstr.*; *Curr. Contents*; *Phys. Chem. Earth Sci.*; *Geo Abstr.*; *Mineral Abstr.*)

Ubiquitous occurrence of basaltic-derived paleosols in the Late Archean Fortescue Group, Western Australia Y. Teitler, P. Philippot, M. Gérard, G. Le Hir, F. Fluteau and M. Ader	1
Global synchronous initiation of the 2nd episode of Sturtian glaciation: SIMS zircon U–Pb and O isotope evidence from the Jiangkou Group, South China Z. Lan, X.-H. Li, Q. Zhang and Q.-L. Li	28
Interaction between the Central Asian Orogenic Belt (CAOB) and the Siberian craton as recorded by detrital zircon suites from Transbaikalia V. Powerman, A. Shatsillo, N. Chumakov, I. Kapitonov and J. Hourigan	39
Zircon U–Pb–Hf isotopes and geochemistry of two contrasting Neoproterozoic charnockitic rock series in Eastern Hebei, North China Craton: Implications for petrogenesis and tectonic setting X. Bai, S. Liu, R. Guo and W. Wang	72
Baltica during the Ediacaran and Cambrian: A paleomagnetic study of Hailuoto sediments in Finland R. Klein, J. Salminen and S. Mertanen	94
Zircon U–Pb geochronology and Nd isotope systematics of the Abas terrane, Yemen: Implications for Neoproterozoic crust reworking events F.G. Yeshanew, V. Pease, M.J. Whitehouse and S. Al-Khribash	106
Archean–Paleoproterozoic crustal evolution of the Ordos Block in the North China Craton: Constraints from zircon U–Pb geochronology and Hf isotopes for gneissic granitoids of the basement C. Zhang, C. Diwu, A. Kröner, Y. Sun, J. Luo, Q. Li, L. Gou, H. Lin, X. Wei and J. Zhao	121
Multi-stage metamorphism in the Rayner–Eastern Ghats Terrane: <i>P–T–t</i> constraints from the northern Prince Charles Mountains, east Antarctica L.J. Morrissey, M. Hand and D.E. Kelsey	137
Age and implications of the phosphatic Birmania Formation, Rajasthan, India N.C. Hughes, P.M. Myrow, N.R. McKenzie, S. Xiao, D.M. Banerjee, D.F. Stöckli and Q. Tang	164
Precise U–Pb baddeleyite age dating of the Usushwana Complex, southern Africa—Implications for the Mesoarchean magmatic and sedimentological evolution of the Pongola Supergroup, Kaapvaal Craton A. Gumsley, J. Olsson, U. Söderlund, M. de Kock, A. Hofmann and M. Klausen	174
Late Ediacaran skeletal body fossil assemblage from the Navalpino anticline, central Spain I. Cortijo, M.M. Mus, S. Jensen and T. Palacios	186
Neoproterozoic quartz monzodiorite–granodiorite association from the Luding–Kangding area: Implications for the interpretation of an active continental margin along the Yangtze Block (South China Block) S.-c. Lai, J.-f. Qin, R.-Z. Zhu and S.-w. Zhao	196
Marine redox variations and nitrogen cycle of the early Cambrian southern margin of the Yangtze Platform, South China: Evidence from nitrogen and organic carbon isotopes D. Wang, U. Struck, H.-F. Ling, Q.-J. Guo, G.A. Shields-Zhou, M.-Y. Zhu and S.-P. Yao	209

(Contents continued on BM II)

CAPTION FOR COVER PHOTOGRAPH

3,243 million-year-old spherules in the Fig Tree Group, Barberton Greenstone Belt, South Africa, formed as a result of large meteorite impacts on the early Earth. The 35-cm-thick spherule bed (S3) is composed of nearly pure spherules produced during the condensation of an impact-produced rock vapor cloud. The estimated diameter of the bolide was 20–50 km. The spherules, 0.5–1.5 mm in diameter in the photo, include silica-(clear), phyllosilicate- (gray), and rutile/anatase-rich (black) varieties; massive and layered types; and a few originally hollow spherules. This is one of four spherule layers in the Barberton Belt, ranging from 3,470–3,243 Ma, that represent the oldest known impact deposits and provide direct evidence for a significant flux of large impactors as late as 3.2 Ga. Photograph: D.R. Lowe



II

(Contents continued from back cover)

Stratigraphy, diagenesis and geological evolution of the Paleoproterozoic Roraima Basin, Guyana: Links to tectonic events on the Amazon Craton and assessment for uranium mineralization potential S.R. Beyer, E.E. Hiatt, K. Kyser, G.L. Drever and J. Marlatt	227
Geochronology of the DeGrussa volcanic-hosted massive sulphide deposit and associated mineralisation of the Yerrida, Bryah and Padbury Basins, Western Australia M.L. Hawke, S. Meffre, H. Stein, P. Hilliard, R. Large and J.B. Gemmell	250
Unraveling crustal growth and reworking processes in complex zircons from orogenic lower-crust: The Proterozoic Putumayo Orogen of Amazonia M. Ibanez-Mejia, A. Pullen, J. Arenstein, G.E. Gehrels, J. Valley, M.N. Ducea, A.R. Mora, M. Pecha and J. Ruiz	285
Paleoarchean sulfur cycling: Multiple sulfur isotope constraints from the Barberton Greenstone Belt, South Africa A. Montinaro, H. Strauss, P.R.D. Mason, D. Roerdink, C. Münker, U. Schwarz-Schampera, N.T. Arndt, J. Farquhar, N.J. Beukes, J. Gutzmer and M. Peters	311

(Abstracts/contents lists published in *Am. Geol. Inst. Bibliogr.*; *Abstr. Bull. Signalétique*; *Chem. Abstr.*; *Curr. Contents*; *Phys. Chem. Earth Sci.*, *Geo Abstr.*; *Mineral Abstr.*)

Late Mesoproterozoic to early Neoproterozoic ridge subduction along southern margin of the Jiangnan Orogen: New evidence from the Northeastern Jiangxi Ophiolite (NJO), South China C.-L. Zhang, H.-B. Zou, Q.-B. Zhu and X.-Y. Chen	1
Paleoproterozoic (ca. 2.1–2.0 Ga) arc magmatism in the Fuping Complex: Implications for the tectonic evolution of the Trans-North China Orogen L. Tang, M. Santosh and X.-M. Teng	16
The Precambrian tectonic evolution of the western Jiangnan Orogen and western Cathaysia Block: Evidence from detrital zircon age spectra and geochemistry of clastic rocks C. Yan, L. Shu, M. Santosh, J. Yao, J. Li and C. Li	33
Evidence of a Paleoproterozoic basement in the Moroccan Variscan Belt (Rehamna Massif, Western Meseta) M.F. Pereira, M. El Houicha, M. Chichorro, R. Armstrong, A. Jouhari, A. El Attari, N. Ennih and J.B. Silva	61
Metamorphic <i>PT</i> path and zircon U–Pb dating of Archean eclogite association in Gridino complex, Belomorian province, Russia X. Li, L. Zhang, C. Wei and A.I. Slabunov	74
Neoproterozoic intraplate crustal accretion on the northern margin of the Yangtze Block: Evidence from geochemistry, zircon SHRIMP U–Pb dating and Hf isotopes from the Fuchashan Complex L. Liu, X. Yang, M. Santosh, S. Aulbach, H. Zhou, J. Geng and W. Sun	97
Textural and paleo-fluid flow control on diagenesis in the Paleoproterozoic Franceville Basin, South Eastern, Gabon O.M. Bankole, A. El Albani, A. Meunier and F. Gauthier-Lafaye	115
Analog modeling of one-way gravitational spreading of hot orogens - A case study from the Svecofennian orogen, Fennoscandian Shield K. Nikkilä, A. Korja, H. Koyi and O. Eklund	135
Provenance characteristics and regional implications of Neoproterozoic, Timanian-margin successions and a basal Caledonian nappe in northern Norway W. Zhang, D. Roberts and V. Pease	153
Genesis of the Paleoproterozoic NICO iron oxide–cobalt–gold–bismuth deposit, Northwest Territories, Canada: Evidence from isotope geochemistry and fluid inclusions P. Acosta-Góngora, S.A. Gleeson, I.M. Samson, L. Corriveau, L. Ootes, B.E. Taylor, R.A. Creaser and K. Muehlenbachs	168
A revised paleomagnetic pole from the mid-Neoproterozoic Liantuo Formation in the Yangtze block and its paleogeographic implications X.-q. Jing, Z. Yang, Y. Tong and Z. Han	194

(Contents continued on BM IV)

CAPTION FOR COVER PHOTOGRAPH

3,243 million-year-old spherules in the Fig Tree Group, Barberton Greenstone Belt, South Africa, formed as a result of large meteorite impacts on the early Earth. The 35-cm-thick spherule bed (S3) is composed of nearly pure spherules produced during the condensation of an impact-produced rock vapor cloud. The estimated diameter of the bolide was 20–50 km. The spherules, 0.5–1.5 mm in diameter in the photo, include silica-(clear), phyllosilicate- (gray), and rutile/anatase-rich (black) varieties; massive and layered types; and a few originally hollow spherules. This is one of four spherule layers in the Barberton Belt, ranging from 3,470–3,243 Ma, that represent the oldest known impact deposits and provide direct evidence for a significant flux of large impactors as late as 3.2 Ga. Photograph: D.R. Lowe



(Contents continued from back cover)

Middle Neoproterozoic (~845 Ma) continental arc magmatism along the northwest side of the Jiangshan-Shaoxing suture, South China: Geochronology, geochemistry, petrogenesis and tectonic implications Z. Liu, Y.-H. Jiang, G.-C. Wang, C.-Y. Ni, L. Qing and Q. Zhang	212
A new ecological model for the ~565 Ma Ediacaran biota of Mistaken Point, Newfoundland J.B. Antcliffe, A.D. Hancy and M.D. Brasier	227
The long-term high-temperature history of the central Namaqua Metamorphic Complex: Evidence for a Mesoproterozoic continental back-arc in southern Africa J. Bial, S.H. Büttner, V. Schenk and P. Appel	243
Mapping the 3D extent of the Northern Lobe of the Bushveld layered mafic intrusion from geophysical data C.A. Finn, P.A. Bedrosian, J.C. Cole, T.D. Khoza and S.J. Webb	279
Paleo- to Mesoarchean TTG accretion and continental growth in the western Dharwar craton, Southern India: Constraints from SHRIMP U–Pb zircon geochronology, whole-rock geochemistry and Nd–Sr isotopes M. Jayananda, D. Chardon, J.-J. Peucat, Tushipokla and C.M. Fanning	295
3806 Ma Isua rhyolites and dacites affected by low temperature Eoarchean surficial alteration: Earth's earliest weathering A.P. Nutman, V.C. Bennett, A.R. Chivas, C.R.L. Friend, X.-M. Liu and F.W. Dux	323
Mid-Neoproterozoic diabase dykes from Xide in the western Yangtze Block, South China: New evidence for continental rifting related to the breakup of Rodinia supercontinent X. Cui, X. Jiang, J. Wang, X. Wang, J. Zhuo, Q. Deng, S. Liao, H. Wu, Z. Jiang and Y. Wei	339

(Abstracts/contents lists published in *Am. Geol. Inst. Bibliogr.*; *Abstr. Bull. Signalétique*; *Chem. Abstr.*; *Curr. Contents*; *Phys. Chem. Earth Sci.*, *Geo Abstr.*; *Mineral Abstr.*)

Formation and tectonic evolution of the khondalite series at the southern margin of the North China Craton: Geochronological constraints from a 1.85-Ga Mo deposit in the Xiong'er shan area N. Li, Y.J. Chen, N.J. McNaughton, X.X. Ling, X.H. Deng, J.M. Yao and Y.S. Wu	1
Neoproterozoic assembly of the Yangtze and Cathaysia blocks: Evidence from the Cangshuipu Group and associated rocks along the Central Jiangnan Orogen, South China Y. Zhang, Y. Wang, Y. Zhang and A. Zhang	18
Short-lived high-temperature prograde and retrograde metamorphism in Shaerqin sapphirine-bearing metapelites from the Daqingshan terrane, North China Craton S.-J. Jiao, J.-H. Guo, L.-J. Wang and P. Peng	31
U–Pb geochronology and paleomagnetism of the Westerbeg Sill Suite, Kaapvaal Craton – Support for a coherent Kaapvaal–Pilbara Block (Vaalbara) into the Paleoproterozoic? T.C. Kampmann, A.P. Gumsley, M.O. de Kock and U. Söderlund	58
Neoproterozoic granitic gneisses in the Chinese Central Tianshan Block: Implications for tectonic affinity and Precambrian crustal evolution Z. Huang, X. Long, A. Kröner, C. Yuan, Y. Wang, B. Chen and Y. Zhang	73
New paleomagnetic results from the Huaibei Group and Neoproterozoic mafic sills in the North China Craton and their paleogeographic implications X. Fu, S. Zhang, H. Li, J. Ding, H. Li, T. Yang, H. Wu, H. Yuan and J. Lv	90
Relating unconformity-type uranium mineralization of the Alligator Rivers Uranium Field (Northern Territory, Australia) to the regional Proterozoic tectono-thermal activity: An illite K–Ar dating approach N. Clauer, J. Mercadier, P. Patrier, E. Laverret and P. Bruneton	107
Phase equilibria and trace element modeling of Archean sanukitoid melts J. Semprich, J.A. Moreno and E.P. Oliveira	122
Taphonomy of the Ediacaran <i>Podolimirus</i> and associated dipleurozoans from the Vendian of Ukraine J. Dzik and A. Martyshyn	139
U–Pb detrital zircon and ³⁹ Ar– ⁴⁰ Ar muscovite ages from the eastern parts of the Karagwe-Ankole Belt: Tracking Paleoproterozoic basin formation and Mesoproterozoic crustal amalgamation along the western margin of the Tanzania Craton C. Koegelenberg, A.F.M. Kisters, J.D. Kramers and D. Frei	147
Paleoproterozoic multistage evolution of the lower crust beneath the southern North China Craton X. Ping, J. Zheng, H. Tang, Q. Xiong and Y. Su	162
Paleoecology of the enigmatic <i>Tribrachidium</i> : New data from the Ediacaran of South Australia C.M.S. Hall, M.L. Droser, J.G. Gehling and M.E. Dzaugis	183
Neoproterozoic active continental margin of the Cathaysia block: Evidence from geochronology, geochemistry, and Nd–Hf isotopes of igneous complexes Y. Xia, X. Xu, G. Zhao and L. Liu	195

(Contents continued on BM II)

CAPTION FOR COVER PHOTOGRAPH

3,243 million-year-old spherules in the Fig Tree Group, Barberton Greenstone Belt, South Africa, formed as a result of large meteorite impacts on the early Earth. The 35-cm-thick spherule bed (S3) is composed of nearly pure spherules produced during the condensation of an impact-produced rock vapor cloud. The estimated diameter of the bolide was 20–50 km. The spherules, 0.5–1.5 mm in diameter in the photo, include silica-(clear), phyllosilicate- (gray), and rutile/anatase-rich (black) varieties; massive and layered types; and a few originally hollow spherules. This is one of four spherule layers in the Barberton Belt, ranging from 3,470–3,243 Ma, that represent the oldest known impact deposits and provide direct evidence for a significant flux of large impactors as late as 3.2 Ga. Photograph: D.R. Lowe



(Contents continued from back cover)

Neoproterozoic metamorphic events along the eastern margin of the East Sahara Ghost Craton at Sabaloka and Bayuda, Sudan: Petrology and texturally controlled in-situ monazite dating S. Karmakar and V. Schenk	217
Distinguishing between local versus regional extension as a control on orogenic gold mineralisation: The new 2.4 Moz Castle Hill Camp, WA J.D. Warren, N. Thébaud, J.M. Miller and S. Micklethwaite	242
Structural architecture of the southern Mount Isa terrane in Queensland inferred from magnetic and gravity data G.P.T. Spampinato, P.G. Betts, L. Ailleres and R.J. Armit	261
Structurally-controlled hydrothermal alteration in the syntectonic Neoproterozoic Upper Ruvubu Alkaline Plutonic Complex (Burundi): Implications for REE and HFSE mobilities S. Decrée, P. Boulvais, C. Cobert, J.-M. Baele, G. Midende, V. Gardien, L. Tack, G. Nimpagaritse and D. Demaiffe	281
Characterization of the Paleoproterozoic Hottah terrane, Wopmay Orogen using multi-isotopic (U-Pb, Hf and O) detrital zircon analyses: An evaluation of linkages to northwest Laurentian Paleoproterozoic domains W.J. Davis, L. Ootes, L. Newton, V. Jackson and R.A. Stern	296

(Abstracts/contents lists published in *Am. Geol. Inst. Bibliogr.*; *Abstr. Bull. Signalétique*; *Chem. Abstr.*; *Curr. Contents*; *Phys. Chem. Earth Sci.*; *Geo Abstr.*; *Mineral Abstr.*)

Precambrian evolution of the Tarim Block and its tectonic affinity to other major continental blocks in China: New clues from U–Pb geochronology and Lu–Hf isotopes of detrital zircons Z. Li, N. Qiu, J. Chang and X. Yang	1
Near-orthogonal deformation successions in the poly-deformed Paleoproterozoic Martimo belt: Implications for the tectonic evolution of Northern Fennoscandia R. Lahtinen, M. Sayab and F. Karell	22
U–Pb SHRIMP detrital zircon ages from the Neoproterozoic Difunta Correa Metasedimentary Sequence (Western Sierras Pampeanas, Argentina): Provenance and paleogeographic implications C.D. Ramacciotti, E.G. Baldo and C. Casquet	39
Secular changes of water chemistry in shallow-water Ediacaran ocean: Evidence from carbonates at Xiaofenghe, Three Gorges area, Yangtze Platform, South China S.V. Hohl, H. Becker, A. Gamper, S.-Y. Jiang, U. Wiechert, J.-H. Yang and H.-Z. Wei	50
The Neoproterozoic ultramafic–mafic complex in the Yinshan Block, North China Craton: Magmatic monitor of development of Archean lithospheric mantle D. Wang, J. Guo, G. Huang and M. Scheltens	80
Grenvillian-aged reworking of late Paleoproterozoic crust of the southern North Australian Craton, central Australia: Implications for the assembly of Mesoproterozoic Australia B.L. Wong, L.J. Morrissey, M. Hand, C.E. Fields and D.E. Kelsey	100
2.24 Ga mafic dykes from Taihua Complex, southern Trans-North China Orogen, and their tectonic implications J. Han, H. Chen, J. Yao and X. Deng	124
Thermotectonic evolution of the western margin of the Yilgarn craton, Western Australia: New insights from ⁴⁰ Ar/ ³⁹ Ar analysis of muscovite and biotite S. Lu, D. Phillips, B.P. Kohn, A.J.W. Gleadow and E.L. Matchan	139
Passive seismological imaging of the Narmada paleo-rift, central India M.R. Kumar, A. Singh, N. Kumar and D. Sarkar	155
Geochemistry of the Krivoy Rog Banded Iron Formation, Ukraine, and the impact of peak episodes of increased global magmatic activity on the trace element composition of Precambrian seawater S. Viehmann, M. Bau, J.E. Hoffmann and C. Münker	165
Petrogenesis of Neoproterozoic adakitic tonalites and high-K granites in the eastern Songpan-Ganze Fold Belt and implications for the tectonic evolution of the western Yangtze Block Q. Chen, M. Sun, X. Long and C. Yuan	181
2.17–2.10 Ga plutonic episodes in the Mineiro belt, São Francisco Craton, Brazil: U–Pb ages, geochemical constraints and tectonics N.S. Barbosa, W. Teixeira, C.A. Ávila, P.M. Montecinos and E.M. Bongiolo	204
Revised Neoproterozoic and Terreneuvian stratigraphy of the Lena-Anabar Basin and north-western slope of the Olenek Uplift, Siberian Platform K.E. Nagovitsin, V.I. Rogov, V.V. Marusin, G.A. Karlova, A.V. Kolesnikov, N.V. Bykova and D.V. Grazhdankin	226

(Contents continued on BM IV)

CAPTION FOR COVER PHOTOGRAPH

3,243 million-year-old spherules in the Fig Tree Group, Barberton Greenstone Belt, South Africa, formed as a result of large meteorite impacts on the early Earth. The 35-cm-thick spherule bed (S3) is composed of nearly pure spherules produced during the condensation of an impact-produced rock vapor cloud. The estimated diameter of the bolide was 20–50 km. The spherules, 0.5–1.5 mm in diameter in the photo, include silica-(clear), phyllosilicate- (gray), and rutile/anatase-rich (black) varieties; massive and layered types; and a few originally hollow spherules. This is one of four spherule layers in the Barberton Belt, ranging from 3,470–3,243 Ma, that represent the oldest known impact deposits and provide direct evidence for a significant flux of large impactors as late as 3.2 Ga. Photograph: D.R. Lowe



(Contents continued from back cover)

Episodic Paleoproterozoic (3.3–2.0 Ga) granitoid magmatism in Yangtze Craton, South China: Implications for late Archean tectonics J.-L. Guo, Y.-B. Wu, S. Gao, Z.-M. Jin, K.-Q. Zong, Z.-C. Hu, K. Chen, H.-H. Chen and Y.-S. Liu	246
Age and hafnium isotopic evolution of the Didesa and Kemashi Domains, western Ethiopia M.L. Blades, A.S. Collins, J. Foden, J.L. Payne, X. Xu, T. Alemu, G. Woldetinsae, C. Clark and R.J.M. Taylor	267
Garnet in cratonic and non-cratonic mantle and lower crustal xenoliths from southern Africa: Composition, water incorporation and geodynamic constraints E. Schmädicke, J. Gose, J. Reinhardt, T.M. Will and R. Stalder	285
The origin and hydrothermal mobilization of carbonaceous matter associated with Paleoproterozoic orogenic-type gold deposits of West Africa B. Kříbek, I. Sýkorová, V. Machovič, I. Knésl, F. Laufek and J. Zachariáš	300
Deep-seated crustal xenoliths record multiple Paleoproterozoic tectonothermal events in the northern North China Craton Y. Su, J. Zheng, Y. Wei, Y. Li, X. Ping and Y. Huang	318
Evolution of a ~2.7 Ga large igneous province: A volcanological, geochemical and geochronological study of the Agnew Greenstone Belt, and new regional correlations for the Kalgoorlie Terrane (Yilgarn Craton, Western Australia) P.C. Hayman, N. Thébaud, M.J. Pawley, S.J. Barnes, R.A.F. Cas, Y. Amelin, J. Sapkota, R.J. Squire, I.H. Campbell and I. Pegg	334

(Abstracts/contents lists published in *Am. Geol. Inst. Bibliogr.*; *Abstr. Bull. Signalétique*; *Chem. Abstr.*; *Curr. Contents*; *Phys. Chem. Earth Sci.*; *Geo Abstr.*; *Mineral Abstr.*)

Stratigraphy of the Late Palaeoproterozoic (~2.03 Ga) Woolly Dolomite, Ashburton Province, Western Australia: A carbonate platform developed in a failed rift basin B. Krapež, S.G. Müller and A. Bekker	1
Diagenetic xenotime dating to constrain the initial depositional time of the Yan-Liao Rift Y.-B. Zhang, Q.-L. Li, Z.-W. Lan, F.-Y. Wu, X.-H. Li, J.-H. Yang and M.-G. Zhai	20
Distinctive compositional characteristics and evolutionary trend of Precambrian glaucony: Example from Bhalukona Formation, Chhattisgarh basin, India S. Banerjee, S. Mondal, P.P. Chakraborty and S.S. Meena	33
The geological roots of South America: 4.1 Ga and 3.7 Ga zircon crystals discovered in N.E. Brazil and N.W. Argentina J.L. Paquette, J.S.F. Barbosa, S. Rohais, S.C.P. Cruz, P. Goncalves, J.J. Peucat, A.B.M. Leal, M. Santos-Pinto and H. Martin	49
Seismic imaging across the Eastern Ghats Belt-Cuddapah Basin collisional zone, southern Indian Shield and possible geodynamic implications K. Chandrakala, O.P. Pandey, A.S.S.R.S. Prasad and K. Sain	56
U–Pb age and Hf isotope composition of detrital zircons from Neoproterozoic sedimentary units in southern Anhui Province, South China: Implications for the provenance, tectonic evolution and glacial history of the eastern Jiangnan Orogen X. Cui, W. Zhu, I.C.W. Fitzsimons, J. He, Y. Lu, X. Wang, R. Ge, B. Zheng and X. Wu	65
The Archean–Paleoproterozoic crustal evolution in the Dunhuang region, NW China: Constraints from zircon U–Pb geochronology and in situ Hf isotopes Y. Zhao, Y. Sun, J. Yan and C. Diwu	83
Long history of a Grenville orogen relic–The North Qinling terrane: Evolution of the Qinling orogenic belt from Rodinia to Gondwana S. Yu, S. Li, S. Zhao, H. Cao and Y. Suo	98
Discovery of Hadean–Mesoarchean crustal materials in the northern Sibumasu block and its significance for Gondwana reconstruction G. Li, Q. Wang, Y. Huang, F. Chen and P. Dong	118
Boninitic metavolcanic rocks and island arc tholeiites from the Older Metamorphic Group (OMG) of Singhbhum Craton, eastern India: Geochemical evidence for Archean subduction processes C. Manikyamba, J. Ray, S. Ganguly, M.R. Singh, M. Santosh, A. Saha and M. Satyanarayanan	138
Neoproterozoic (ca. 820–830 Ma) mafic dykes at Olympic Dam, South Australia: Links with the Gairdner Large Igneous Province Q. Huang, V.S. Kamenetsky, J. McPhie, K. Ehrig, S. Meffre, R. Maas, J. Thompson, M. Kamenetsky, I. Chambefort, O. Apukhtina and Y. Hu	160
Deep-water seep-related carbonate mounds in a Mesoproterozoic alkaline lake, Borden Basin (Nunavut, Canada) K.E. Hahn, E.C. Turner, M.G. Babechuk and B.S. Kamber	173

(Contents continued on BM II)

CAPTION FOR COVER PHOTOGRAPH

3,243 million-year-old spherules in the Fig Tree Group, Barberton Greenstone Belt, South Africa, formed as a result of large meteorite impacts on the early Earth. The 35-cm-thick spherule bed (S3) is composed of nearly pure spherules produced during the condensation of an impact-produced rock vapor cloud. The estimated diameter of the bolide was 20–50 km. The spherules, 0.5–1.5 mm in diameter in the photo, include silica-(clear), phyllosilicate- (gray), and rutile/anatase-rich (black) varieties; massive and layered types; and a few originally hollow spherules. This is one of four spherule layers in the Barberton Belt, ranging from 3,470–3,243 Ma, that represent the oldest known impact deposits and provide direct evidence for a significant flux of large impactors as late as 3.2 Ga. Photograph: D.R. Lowe



(Contents continued from back cover)

Generation of felsic crust in the Archean: A geodynamic modeling perspective E. Sizova, T. Gerya, K. Stüwe and M. Brown	198
Petrogenesis and tectonic implications of the iron-rich tholeiitic basalts in the Hutuo Group of the Wutai Mountains, Central Trans-North China Orogen L. Du, C. Yang, D.A. Wyman, A.P. Nutman, Z. Lu, L. Zhao, W. Wang, H. Song, Y. Wan, L. Ren and Y. Geng	225
Stratigraphic position of the Ediacaran Miaohe biota and its constraints on the age of the upper Doushantuo $\delta^{13}\text{C}$ anomaly in the Yangtze Gorges area, South China Z. An, G. Jiang, J. Tong, L. Tian, Q. Ye, H. Song and H. Song	243
Zircon U–Pb–Hf isotope systematics and geochemistry of Helong granite-greenstone belt in Southern Jilin Province, China: Implications for Neoproterozoic crustal evolution of the northeastern margin of North China Craton B. Guo, S. Liu, J. Zhang and M. Yan	254
Newly discovered Neoproterozoic diamictite and cap carbonate (DCC) couplet in Tarim Craton, NW China: Stratigraphy, geochemistry, and paleoenvironment B. Wen, D.A.D. Evans, Y.-X. Li, Z. Wang and C. Liu	278
Metamorphic P–T paths and Zircon U–Pb age data for the Paleoproterozoic metabasic dykes of high-pressure granulite facies from Eastern Hebei, North China Craton Z. Duan, C. Wei and J. Qian	295
Late-Neoproterozoic ultrahigh-temperature metamorphism in the Highland Complex, Sri Lanka P.L. Dharmapriya, S.P.K. Malaviarachchi, M. Santosh, L. Tang and K. Sajeev	311

